A conceptual framework for understanding longwave cloud effects on climate sensitivity

Lukas Kluft[1], Bjorn Stevens[1], Manfred Brath[2], and Stefan A. Buehler[2]

[1]Max Planck Institute for Meteorology, Hamburg, Germany
[2]Center for Earth System Research and Sustainability (CEN), Meteorological Institute, Universität Hamburg, Hamburg, Germany

Correspondence: Lukas Kluft (lukas.kluft@mpimet.mpg.de)

Abstract. We add idealized clouds into a single column model and show that the cloud radiative effects as observed from satellites can be reproduced by a combination of high and either low or mid-level clouds. To quantify all-sky climate sensitivity we adopt the "fixed-cloud-albedo" ansatz as the null hypothesis for the climate sensitivity. Our ansatz assumes an understanding of how clouds distribute themselves in temperature space, but assumes no change in cloud albedo. Drawing only distributions which match the cloud radiative effects of present day observations yields a mean fixed-albedo (also keeping surface albedo fixed) climate sensitivity of $2.2\,\mathrm{K}$, slightly smaller than its clear-sky value. This small number arises from two compensating effects: the dominance of cloud masking of the radiative response, primarily by mid-level clouds which are assumed not to change with temperature, and a reduction of the radiative forcing due to masking effect by high clouds. Giving more prominence to low-level clouds, which are assumed to change their temperature with warming, reduces estimates of the fixed-albedo climate sensitivity to $2.0\,\mathrm{K}$. This provides a baseline to which changes in surface albedo, and a believed reduction in cloud albedo, would add to.

1 Introduction

The cloud-radiative effect is a significant contributor to Earth's radiation balance (Hartmann and Short, 1980; Ramanathan et al., 1989). In the net it leads to a cooling of Earth's surface as the contribution of clouds to the planetary albedo, through scattering of visible radiation, is larger than their greenhouse effect, arising from their absorption of terrestrial radiation (Loeb et al., 2018). A stronger cloud albedo effect is expected because the minimum temperature of the troposphere, and hence clouds, is much larger than zero, which more tightly bounds the cloud greenhouse effect. This gives changes in cloud albedo greater scope for influencing the climate sensitivity, and explains why they are the subject of more study (Ceppi et al., 2017).

Whereas cloud albedo effects arise from either changes in cloud microphysical properties and or spatial extent, cloud greenhouse effects also depend on cloud-top temperature. This means that even under the ansatz of a fixed cloud albedo, the mere manner by which clouds distribute themselves in temperature space may influence Earth's equilibrium climate sensitivity. Two effects can be identified, and respectively correspond to masking of the radiative response to forcing, or warming: For the former, high-clouds mask the radiative forcing in spectral regions (wave-numbers) where CO_2 emissions would otherwise arise from regions below the clouds. At these wave-numbers, and in these situations, the changing emission height arising from

25 an increase in CO_2 will not be apparent at the top of the atmospheres – clouds get in the way. For the latter, clouds modify the radiative response to warming, by masking of emissions in the spectral region known as the atmospheric window and by unmasking parts of the spectral response that they would have otherwise masked, or which would have been masked by water vapor (McKim et al., 2021; Jeevanjee, 2023; Stevens and Kluft, 2023). The cloud masking of CO_2 forcing is well appreciated and accounted for in the literature (Myhre et al., 1998); masking or unmasking of the clear-sky spectral response (Stevens and 30 Kluft, 2023) is not.
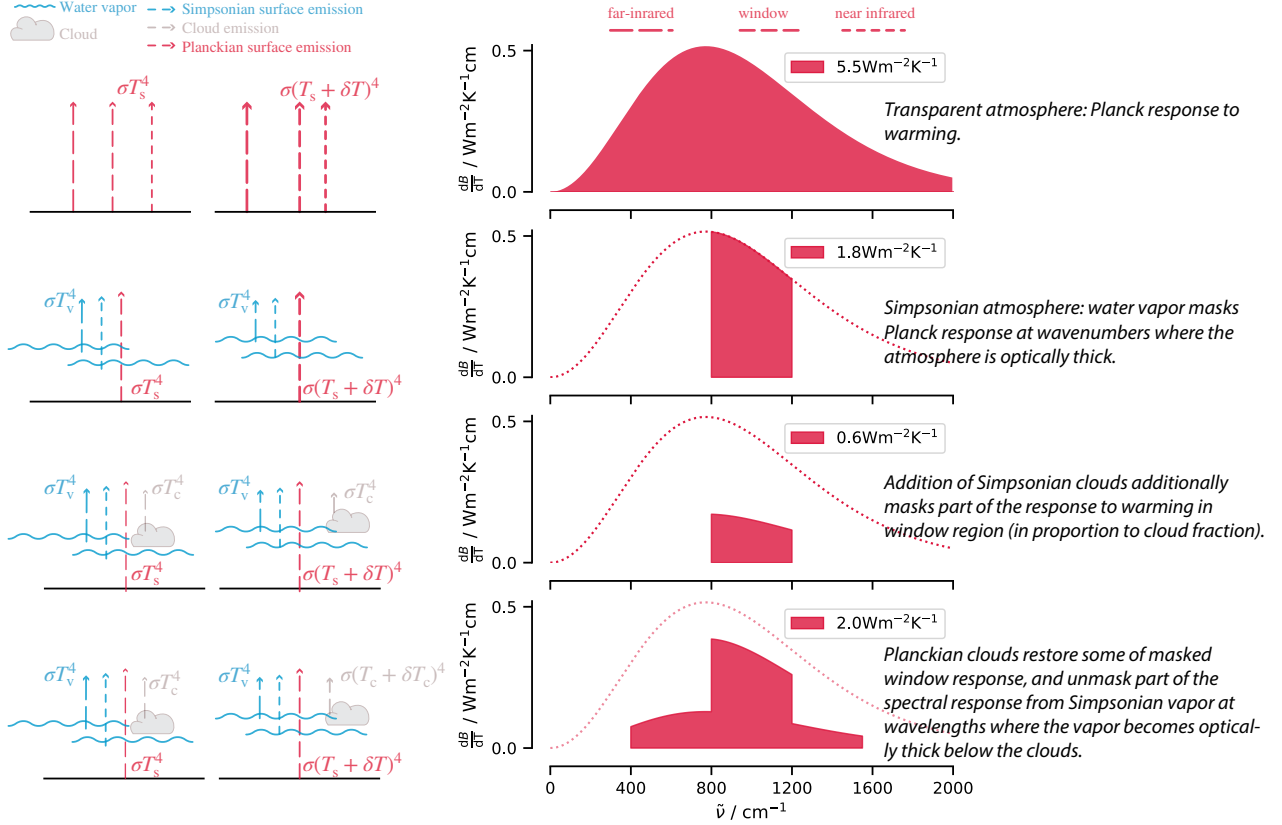
Figure 1. Conceptual framework showing how Simpsonian clouds and water vapor mask the radiative response at wavenumbers where they control the emission to space, and how part of the spectral response is restored from Planckian clouds.

The basic idea of cloud masking is illustrated with the help of the schematic in Fig. 1. For simplicity the schematic leaves out the effects of CO_2 and other long-lived greenhouse gases (see, e.g., Raghuraman et al., 2024). Later, in our more detailed computations, these effects are included. We define the atmospheric window as the range of wavenumbers ($800\,\mathrm{cm^{-1}}$–$1200\,\mathrm{cm^{-1}}$) where the atmosphere is optically thin through the entire column. Outside of this window, emission of radiant energy to space 35 arises from water vapor (as well as from CO_2 or other long-lived greenhouse gases, were they to be considered). In these regions, the assumption of fixed relative humidity means that the optical thickness of the atmosphere, as measured downward

from the top-of-the-atmosphere, depends on temperature, and hence emissions will not change with surface warming. We refer to this as a Simpsonian response (Ingram, 2010; Jeevanjee et al., 2021), which can be conceptualized as a spectral masking of the Planckian response that would otherwise arise from the surface (Fig. 1, second row). Clouds, unlike water vapor, are

40   gray across the thermal infrared. They thus control emissions at wavenumbers where the clear-sky emission would otherwise originate below them. Whether, and how much, they contribute to the radiative response to warming then depends on how or if they warm with the surface. Clouds which maintain a fixed temperature (Simpsonian clouds) mask the spectral response that otherwise would have been expected in the window – reducing the radiative response to surface warming. Clouds that warm with the surface (Planckian clouds) substitute for the surface response within the window. If the change in cloud temperature

45   is equal to the change in the surface temperature, then this mimics the surface response, albeit somewhat weakened by virtue of the clouds being at lower temperatures. Outside of the window, at wavenumbers where the emission height of water vapor lies below the clouds, the warming clouds can reclaim part of the spectral response which would have otherwise been masked by water vapor (Stevens and Kluft, 2023), as shown in the last row of Fig. 1.

Understanding the radiative effect of how clouds distribute themselves in temperature space is a pre-requisite to understand-

50   ing the climate sensitivity. As these effects temper the radiative forcing from greenhouse gases and the radiative response to warming, even in the case when the spatial coverage and microphysical properties of clouds do not change with warming. Previous studies of course include these effects. But rarely are they separated from the clear-sky response. For instance, a common approach to disentangle the cloud feedback is the partial radiative perturbation (PRP) method (Colman, 2003; Soden and Held, 2006). This method performs radiative transfer calculations with different atmospheric fields (e.g. temperature, humidity,

55   clouds) independently varied, with the idea that this quantifies their impact on the radiation budget. Doing so differentiates the effects of changing different variables in coupled models, but ignores the cross-dependencies between variables. As a result the contribution to the radiative response from water vapor, as estimated by the PRP method, will depend on the assumed distribution of clouds; likewise adding and subtracting a given distribution of clouds will give different answers depending on the background distribution of water vapor.

60   In this study we follow Stevens and Kluft (2023) to explicitly account for the masking and unmasking of the spectral response of outgoing radiant energy to surface warming, or CO_2 forcing, under the fixed cloud-albedo ansatz. We begin by providing a precise description of the atmospheric thermodynamic structure, including its clouds, and how this will change with warming. We then calculate the changes in the irradiances with surface warming (or CO_2 forcing) for an atmosphere with and without clouds. Precision of description is facilitated by the use of the single column model `konrad` (Kluft et al.,

65   2019; Dacie et al., 2019), under the fixed cloud-albedo ansatz. That is we assume that spatial coverage of clouds, and their microphysical properties, do not change with warming. Our approach extends a growing literature using simple models under well defined limits to better understand the climate sensitivity of a cloud-free atmosphere, (e.g., Koll and Cronin, 2018; Seeley and Jeevanjee, 2021; Kluft et al., 2021; Jeevanjee et al., 2021; Jeevanjee, 2023; Feng et al., 2023; Koll et al., 2023; Roemer et al., 2023; Stevens and Kluft, 2023), to include the effects of clouds. Using a single column model in this manner is admittedly

70   simplistic, but because the radiative response varies linearly with the main state variables (Koll and Cronin, 2018; Bourdin et al., 2021; Kluft et al., 2021), the response of the mean state has proven to be quantitatively informative of the mean response to a

spatially varying state. More fundamentally our approach allows for a transparency of reasoning, which aids the interpretation of results from more complex settings, and as such is fundamental for understanding **?**.

The manner of our calculations is provided in section 2. In Section 3 we discuss the simulated cloud-radiative effect in present-day conditions as well as the effect of prescribed cloud changes to warming. Section 4 discusses in which aspects our perspective on cloud feedbacks differ or accord with existing frameworks. Section 5 summarizes the conclusions of our study.

2 Modeling the effects of clouds in one dimension

We quantify the radiative effect of clouds using `konrad`, a python based one-dimensional radiative-convective equilibrium (RCE) model (Kluft et al., 2019; Dacie et al., 2019). Clouds at three levels are considered.

It is doubtful if one can unambiguously construct a "global cloud scene" that can be used within `konrad` to best represent cloud effects on the radiative response to warming or forcing. Many of the physical properties of clouds are still poorly quantified. And even if they were well known, the aggregation of these properties for application in a simple one-dimensional model would entail ambiguity, as different representations might be better adapted to different purposes. Hence we approach the problem functionally, by creating a large ensemble of plausible cloud properties for the three layers of clouds to be considered, and selecting configurations consistent with global mean cloud-radiative effects as observed from space (CERES, Loeb et al., 2018). Both the full ensemble of cloud properties and the plausible sub-sample are then used to quantify the cloud masking effect on the radiative forcing, and their masking/unmasking effect on the radiative response to warming

Calculations with `konrad` are preformed by prescribing the surface temperature. The tropospheric temperature profile is adjusted to a moist adiabat corresponding to that surface temperature. Above the convective-top, which is the upper-most level that requires convective adjustment, the temperature profile is equilibrated into a radiative equilibrium which allows us to capture changes in cold-point temperatures. This approach greatly reduces the computational burden as it avoids the need to equilibrate the surface temperature (Romps, 2020). The relative humidity RH is modeled as a C-shaped profile, as roughly observed in the tropics. The RH profile is kept constant in temperature space, thus adjusting it's vertical structure as the troposphere expands (Romps, 2014). For simplicity, we approximate the RH profile using a piecewise linear function of temperature T. It is specified to have a value of $80\,\%$ at $T \geq 283\,\mathrm{K}$, decreasing to a minimum of $40\,\%$ at $250\,\mathrm{K}$ and increasing back to a value of $80\,\%$ at $T \leq 200\,\mathrm{K}$.

All-sky fluxes are calculated using a two-stream correlated-k representation of radiative transfer, RRTMG (Mlawer et al., 1997). Our previous work has shown RRTMG to compare well against line by line calculations within this same framework, and for the temperature ranges considered here (Kluft et al., 2021). RRTMG computes fluxes for completely overcast or clear-sky scenes. In overcast scenes, clouds are represented in terms of their pressure and temperature, optical depth, single scattering albedo and asymmetry parameter, with the optical properties represented as a function of an assumed cloud phase, condensate burden, and effective radius. All sky fluxes are constructed by weighted averages between clear and overcast scenes depending on the fractional weight of each.

The three layers of clouds are endowed with distinct physical properties and behaviours as follows. A low-level cloud-layer is introduced to represent boundary layer clouds, and its cloud-top temperature changes following a fixed anvil pressure (FAP), which due to the assumption of the moist adiabat means they will warm slightly more than the surface[1]; a mid-level cloud layer is introduced at the melting level and is assumed to maintain a fixed anvil temperature (FAT); and a high-level cloud layer following the proportionally higher anvil temperature (PHAT) hypothesis, in which clouds are tied to the level of the maximum of the radiatively driven convergence in clear skies (Zelinka and Hartmann, 2010; Bony et al., 2016). This approach allows the cloud-altitude to be precisely defined for different background climates. Therefore, we can use two simulations with differing surface temperatures $T_s = 285\,\text{K}$ and $291\,\text{K}$ to compute the radiative feedback including the cloud-altitude feedback. The somewhat high value of $\Delta T_s = 6\,\text{K}$ is intended to give a clear signal of changes in cloud top height, which can only be changed by full model levels.

We assume that the overlap among clouds in different layers is random, which defines 2^3 different cloud configurations – each of which can lead to markedly different cloud radiative effects. In global circulation models (GCMs), this variability is parameterised by, e.g. the Monte-Carlo Independent Column Approximation (McICA, Pincus et al., 2003). This is effective when the radiation scheme is called often in time, as the sample noise is unbiased and averages out with high-temporal sampling. For our purposes, the limited number of cloud layers, and hence the smallness (2^3) of the configuration space allows for a simpler approach. Let $i \in \{1\ldots8\}$ index each cloud combination, such that $i = 1$ denotes clear skies, $i = 2$ denotes only high clouds, and so on, as illustrated in Fig. 2. The probability of a given combination of clouds is then given as

$$P_i = \prod_{j=1}^{3} P_{ij} \tag{1}$$

with P_{ij} being the probability that cloud-layer j is seen in cloud combination i, it can be expressed as follows:

$$P_{ij} = |1 - p_j - c_{ij}| \tag{2}$$

with binary cloud flag c_{ij}, which states if cloud layer j is present in combination i, and assumed cloud fraction p_j. The resulting weight P_i quantifies the probability of a given cloud combination based on the cloud fraction of the participating cloud layers. The all-sky radiative fluxes are then given by the weighted average of the individual cloud-overcast scenes (Figure 2).

$$F = \sum P_i F_i. \tag{3}$$

To perform the calculations we also need to make a choice for the cloud fraction, the integrated condensate path for each cloud layer, and the effective radius. The particle phase, which influences how these physical properties are translated into optical properties is prescribed for each layer, with low- and mid-level clouds being treated as liquid and high clouds being treated as ice, and with no change in the phase of the different layers with warming. We account for ambiguities in the cloud description by using a large Monte-Carlo ensemble (MCE) from which we randomly drawing parameter values from values

---

[1]We use the term anvil liberally to refer to the cloud top region, as it allows consistency with existing terminology for high clouds, which also are not strictly anvil shaped.
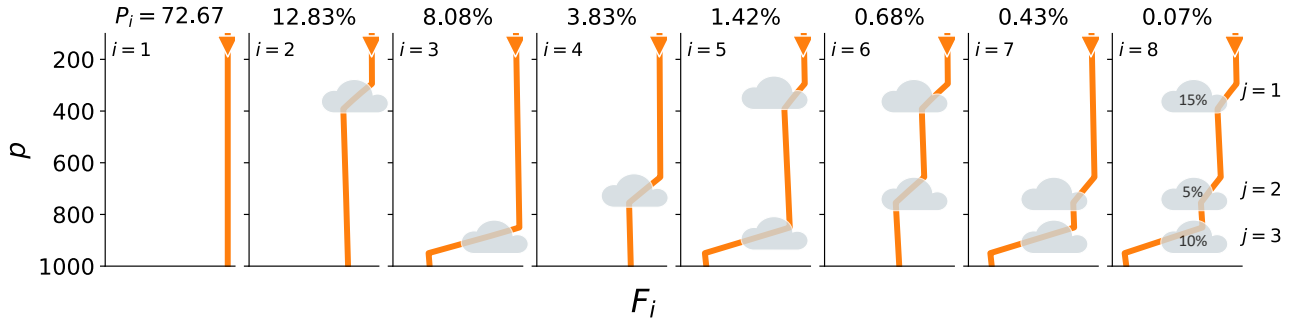
Figure 2. Schematic of all possible cloud-layer combinations i in a trimodal cloud distribution. In addition, the different impact on the downwelling shortwave flux is shown as orange line. The percentages on top state the probability P_i for each cloud-layer combination assuming random overlap and exemplary cloud fractions (shown in the right most panel).

taken from a uniform prior distribution over the specified range. These properties are then held constant from the control and perturbed simulations. The combination of specified but constant cloud fraction, condensate path, effective radius and cloud
135   phase, together with the chosen overlap assumption thus define our fixed cloud-albedo ansatz.

Table 1 lists the range of possible values for each cloud property, from which we construct the MCE. We perform $32\,768$ simulations, each of which comprises sixteen radiative transfer calculations (once for the warm and control temperature for each of the 8 configurations), with parameters chosen randomly from the parent distribution. The result is an ensemble of $32\,768$ cloud scenes that describe the all-sky radiation budgets following the prior distribution of cloud parameters. Many of
140   these scenes will, however, not result in plausible representations of Earth's top of the atmosphere radiation budget, as observed from satellite. Therefore, we construct an a posteriori distribution by sub-sampling the ensemble to find cloud configurations whose cloud-radiative effect (CRE) is consistent with satellite observations. This defines a plausible set of cloud scenes, which we then use to quantify various cloud-radiative metrics in both the present and a warmer climate.

3   Cloud radiative effects

145   ### 3.1   The current climate

In a first step, we quantify how the presence of clouds impacts Earth's radiant energy budget for the control temperature, and use these effects to sample a plausible parameter range for the prescribed clouds. Cloud radiative effects are compared to the summary values for the July 2005–June 2015 period as provided by the Clouds and Radiant Energy Systems (CERES) EBAF Ed4.0 product (Loeb et al., 2018, Tab. 5).
150   Figure 3 presents the longwave, shortwave, and net CRE for the full ensemble (light colors). Unsurprisingly, values for the net CREs and its components spread across a very large range of values. For example, the CRE_{net} can reach values between

$-83\,\mathrm{W\,m^{-2}}$ and $28\,\mathrm{W\,m^{-2}}$. That the ensemble mean is in good agreement with the CERES data suggests that the uniform distributions for the variable parameters were centered around sensible values.

As a next step, we sub-sample the full ensemble to select cloud configurations in which all three CRE values are within $\pm 5\,\mathrm{W\,m^{-2}}$ of the CERES values at the top-of-the-atmosphere – which we refer to as "plausible" values. Tests with narrower acceptance showed no qualitative difference but greatly reduced the output statistics. Even with this relatively loose constraint on acceptable values of the SW ($-45.8\,\mathrm{W\,m^{-2}}$), LW ($27.9\,\mathrm{W\,m^{-2}}$) and net CRE ($-17.9\,\mathrm{W\,m^{-2}}$), requiring all three to be satisfied reduces the ensemble to 786 out of 32786 cloud scenes (about $2.4\,\%$). Parameter distributions for the subset of parameters leading to plausible CRE are described by the 5th, 50th, and 95th percentiles of their distributions and listed in Table 2. The a posteriori distributions show that the CRE from CERES most strongly constrains the property of high-level clouds.

Since the effective parameters found to capture the observed CRE are found to be similar to parameters characteristic to observed clouds, it is justified to use an effective cloud to model the globally averaged effect of broad cloud distributions. The average cloud fraction is $18\,\%$ for high clouds, $20\,\%$ for mid-level clouds and $17\,\%$ for low clouds, which are not unreasonable values. The coverage of mid-level clouds is higher than expected, but could be interpreted as representative of cloud populations in the mid-latitudes. The plausible range for the mid-level and low-level cloud parameters is not substantially reduced relative to their initial distributions, this might be indicative of the capability of the two cloud types to compensate for one another.

To test the possibility of compensation we further investigate the impact of individual cloud layers by performing three additional sets of simulations. In each of these we omit one of the three cloud layers. Results are presented in Figure 3. The strongest impact is seen in the simulation without high clouds. In absence of high clouds, which are characterized by their cold cloud-top, the longwave CRE almost vanishes. As a result, the net CRE is much more negative (about $-40\,\mathrm{W\,m^{-2}}$ on average), and can no longer be reconciled with the CERES data, and thus we do not plot bold lines in Figure 3 for the "no high cloud" case. The calculations also confirm the ability of increased low-level clouds to compensate for mid-level clouds and vice versa. Table 2 further demonstrates that for two cloud layers, the cloud parameters of the lower cloud layers become more constrained than for the case of three layers. In the absence of either the mid- or low-level clouds, Figure 3 indicates that strongly negative $\mathrm{CRE_{SW}}$ are no longer possible, which makes it more difficult to find samples that reproduce the observed $\mathrm{CRE_{SW}}$, increasingly so in the absence of low clouds.

We conclude that a single column model with an idealized trimodal cloud distribution is able to produce CREs that are in good agreement with the best available observations of Earth's radiant energy budget. Our calculations demonstrate that the presence of high clouds is essential for a realistic longwave CRE. Low- and mid-level clouds while important, act in a similar way, making it easier for them to compensate for one another. The CRE at the top-of-the-atmosphere is unable to distinguish between low-level and mid-level cloud amounts. This limitation has significant implications for understanding how the system responds to global warming, as modeled in our study. Specifically, our model shows that mid-level clouds mask the radiative response to warming, whereas low-level clouds, which warm in tandem with the surface (as prescribed in the model), are also effective at enhancing the spectral response to warming.
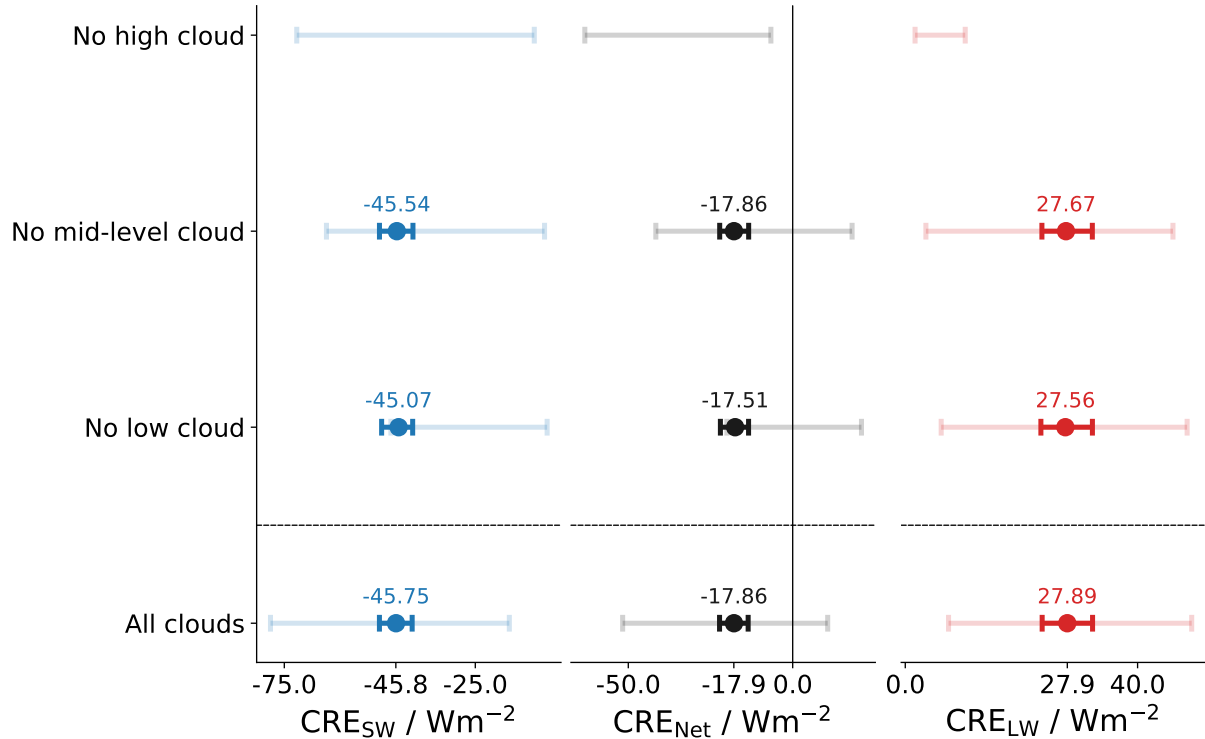
Figure 3. Distribution of the shortwave cloud-radiative effect $\mathrm{CRE_{SW}}$, the net cloud-radiative effect $\mathrm{CRE_{Net}}$, the longwave cloud-radiative effect $\mathrm{CRE_{LW}}$. The faded lines depict the 5 %–95 % interval of all possible CRE values in the full ensemble. The bold lines show the same range, but for a plausible subsample that is in a $\pm 5\,\mathrm{W\,m^{-2}}$ range around the mean values from the CERES satellite observations (given as tick labels on the x-axis). Different "rows" of the figure show results for different simulations, in which certain cloud layers were turned off (e.g. the first for describes a simulation with all but high clouds).

3.2 Response to surface warming

In this section we quantify how our representation of clouds modifies the model's clear-sky response to forcing, the radiative response to warming, and their quotient, the climate sensitivity.

In exploring how clouds with both a fixed coverage, and a fixed albedo (and hence phase), affect the estimate of climate sensitivity we are exploring a form of state dependence, with the cloud distribution being the important state parameter. Past studies, using methods like PRP, would have subsumed these effects into estimates of the clear-sky sensitivity. Our approach allows for a more full accounting of clouds, and by implication allows us to assess how errors in the distribution of clouds, or estimates of changes in cloud temperature, will effect estimates of climate sensitivity.

The calculations involve additional simulations, based on the MCE of cloud scenes. In a first step, we double the CO_2 concentration while keeping a fixed $T_{\mathrm{s}} = 288\,\mathrm{K}$. After letting the stratosphere adjust to the new gaseous composition, we can

directly quantify the adjusted radiative forcing as

$$\Delta F = F_{2\times CO_2} - F_{CO_2} \tag{4}$$

with F_x being the outgoing longwave radiation for a CO_2 mixing ratio x.

We find that clouds reduce the radiative forcing by about $0.7\,\mathrm{W\,m^{-2}}$, or by about $15\,\%$ of the clear-sky value of $4.5\,\mathrm{W\,m^{-2}}$ (see bottom row of Figure 4). This masking is solely done by high clouds, because the cloud needs to be located above the emission height of CO_2 to effectively mask the radiative forcing. In the absence of high clouds ΔF is close to the clear-sky value (see top row of Figure 4). By constraining our MCE to plausible cloud combinations (bold lines), we find that the reduction in ΔF is a robust signal and, on its own, would reduce the fixed-albedo climate sensitivity by about $0.5\,\mathrm{K}$.

In a second step, we estimate how clouds influence the radiative response to forcing, λ. We quantify this by repeating our simulations at $T_s = 285\,\mathrm{K}$ and $291\,\mathrm{K}$. Using the two sets of simulations at different T_s, we define the feedback parameter as

$$\lambda = \frac{F_{291\,\mathrm{K}} - F_{285\,\mathrm{K}}}{6\,\mathrm{K}}, \tag{5}$$

with F_T denoting the net irradiance at the top-of-atmosphere for the given temperature T.

In each of the simulations the different cloud levels adjust their cloud-top altitude based on the thermodynamic profiles of the atmosphere (see Section 2). This means that low-level clouds remain at the same pressure level, mid-level clouds move upward following the melting level, and high-level clouds move upward following the level where the divergence of the radiatively driven subsidence maximizes. As a result both high and low-clouds warm with the surface, high-level clouds somewhat less so, while mid-level clouds remain at the same temperature. The different behavior of mid- and low-level clouds helps quantify to what extent an uncertain temperature response of clouds to surface warming affects the sensitivity of the system to forcing – effectively providing a first estimate of uncertainty introduced by clouds, even if their coverage remains unchanged.

Figure 4b presents λ. Clouds reduce the radiative response to warming, increasing λ from its clear-sky value of $-1.9\,\mathrm{W\,m^{-2}\,K^{-1}}$ to $-1.7\,\mathrm{W\,m^{-2}\,K^{-1}}$. This alone would result in an increase of the equilibrium climate sensitivity $\mathcal{S}$. This effect, however, is less than that of changes in ΔF, which reduces from $4.5\,\mathrm{W\,m^{-2}}$ to $3.7\,\mathrm{W\,m^{-2}}$. Hence, under the fixed cloud-albedo ansatz, clouds slightly reduce $\mathcal{S}$ relative to its clear-sky value. Following the arguments of Stevens and Kluft (2023) this is expected to the extent that clouds unmask parts of the spectral response to warming that would otherwise be masked by water vapor. Comparing the no mid-level versus the no low-level cloud response shows that low-level clouds are responsible for this unmasking, as in their absence the radiative response to warming is much smaller, and $\mathcal{S}$ increases by $0.2\,\mathrm{K}$ (Fig. 4 over its clear-sky value of $2.3\,\mathrm{K}$). Conversely, in the absence of mid-level clouds, the increase in low-level clouds, which in our model warm slightly more than the surface, enhances the radiative response to warming reducing $\mathcal{S}$ by $0.3\,\mathrm{K}$ relative to its clear-sky value.

In summary, the net effect on λ is sufficient to balance the reduction in ΔF resulting in an equilibrium climate sensitivity $\mathcal{S} = -\Delta F/\lambda$ in the range of $1.94\,\mathrm{K}$–$2.56\,\mathrm{K}$. This range encompasses the clear-sky value of $2.3\,\mathrm{K}$, but more often leads to less rather than more warming. This outcome arises because, in our ansatz, the cloud masking effect on ΔF largely compensates that on λ, while the unmasking effect only influences λ, thereby reducing $\mathcal{S}$.
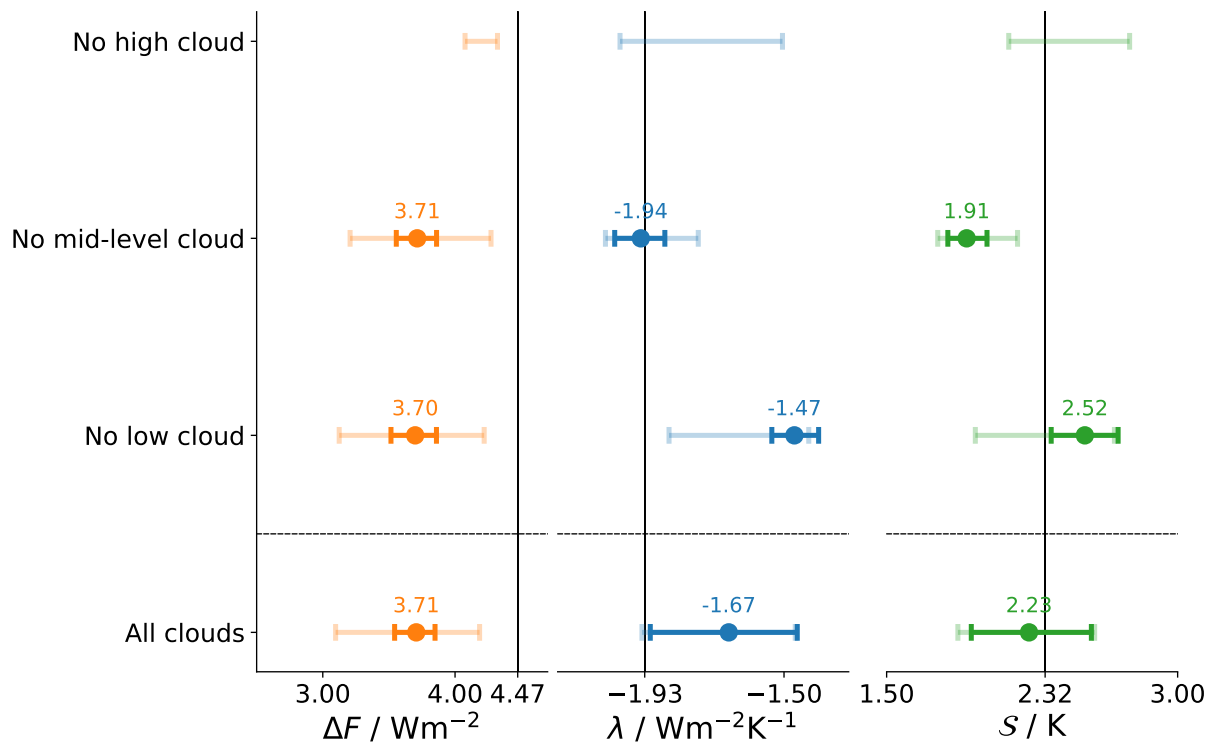
Figure 4. Distribution of the adjusted radiative-forcing ΔF, the climate feedback parameter λ, the equilibrium climate sensitivity $\mathcal{S}$. The faded lines depict the $5\,\%$–$95\,\%$ interval of all possible CRE values in the full ensemble. The bold lines show the same range, but for a plausible subsample that is in agreement with satellite observations. Vertical lines mark the respective value at clear-sky conditions. Different "rows" of the figure show results for different simulations, in which certain cloud layers were turned off (e.g. the first for describes a simulation with all but high clouds).

4 Discussion

Readers familiar with traditional cloud feedback analyses might be confused by the estimates of cloud masking in the present study, as compared to estimates in the earlier literature (Colman, 2003; Soden et al., 2008; Yoshimori et al., 2020). These difference reflect differences in how masking is defined. In the earlier studies, cloud masking was introduced to separate the effect of "fixed clouds" on the radiative response due to changes in non cloud quantities (temperature, water vapor, etc), from changes that could be attributed to clouds not being "fixed". In the earlier studies "fixed" meant fixed in height or pressure. In a warmer climate, "fixing" clouds in this manner results in more emission from clouds, which is a curious way to think about no change, as it implies a strong enhancement of overall radiative response by "fixed clouds". This curious behavior was then more or less canceled once clouds are allowed to change their temperature. A large negative cloud masking was compensated for by a large positive cloud feedback. This side effect of an artificial assumption as to what constitutes a "fixed cloud" is precisely what Yoshimori et al. (2020) set out to address through their introduction of the T-FRAT (thermal radiative damping with fixed

relative humidity and anvil temperature) framework. In that framework they identify a small positive cloud feedback, implying that clouds warm more than expected for a fixed anvil temperature. This is consistent with the response of high-clouds in the present study. But here too quantitative comparison is difficult, as in contrast to our framework, which defines the effect of fixed-albedo clouds relative to cloud-free response, T-FRAT quantifies the effect of cloud changes relative to what would have occurred had clouds maintained a fixed temperature.

One should avoid attaching too much precision to the numbers arising from our calculations. While we can think of myriad ways in which fixed-albedo clouds might distribute themselves in temperature space differently than we have assumed, we don't see arguments that would be indicative of a systematic positive or negative bias. Even without accounting for additional sources of uncertainty in our implementation of the fixed-albedo ansatz – for instance in how cloud overlap, low-cloud warming, or the tendency to place lots of clouds in the middle troposphere where they are given properties that strongly reduce the radiative response – considerable uncertainty arises merely from the configuration of clouds. This effect leads to an uncertainty of approximately $0.5\,\mathrm{W\,m^{-2}\,K^{-1}}$ in λ, which quantifies what Yoshimori et al. (2020) called the cloud climatological effect in our model. Observations, combined with three dimensional calculations using reanalyses, similar to the approach Gloeckner et al. (in press 2025) used to study the clear-sky feedback could help reduce this uncertainty, or at least quantify the adequacy of existing cloud climatologies for this purpose.

Even under the fixed cloud-albedo ansatz clouds can contribute to changes in planetary albedo through their ability to mask surface albedo changes. Pistone et al. (2014) estimate an all-sky radiative response to surface albedo changes that is $5/8$ths of the clear-sky response – although some of this is likely associated with changes in cloud cover. Thus an all-sky surface albedo radiative response to surface albedo changes of $0.35\,\mathrm{W\,m^{-2}\,K^{-1}}$ (Forster et al., 2021) implies a clear-sky surface albedo contribution to the radiative response of $0.56\,\mathrm{W\,m^{-2}\,K^{-1}}$. Accounting for these changes in our null-hypothesis for climate sensitivity gives the best estimate of the fixed atmosphere-albedo clear-sky sensitivity to $3.26\,\mathrm{K}$, and the fixed atmosphere-albedo all-sky sensitivity to $2.8\,\mathrm{K}$. This demonstrates that fixed-albedo clouds reduce the climate sensitivity even more when surface albedo changes are incorporated.

5   Conclusions

We propose a model for cloud-altitude changes in a warming climate, and use this to calculate the climate sensitivity under the fixed cloud-albedo ansatz. Our model allows different cloud types to respond to surface warming in distinct ways: low-level clouds are assumed to be tied to a fixed pressure, mid-level clouds to the freezing level, and high-level clouds to the level of maximum clear-sky subsidence divergence. We add this conceptual representation of clouds to the one-dimensional RCE model `konrad` to quantify how, if they were to behave in the manner posited, they would affect the radiative response to forcing. The model helps clarify both how cloud temperature changes, and how cloud temperature changes of different cloud types, influence the climate sensitivity even under the ansatz of a fixed cloud-albedo.

Satellite observations show that the presence of cloud cools the current climate by adding a net CRE of about $-17\,\mathrm{W\,m^{-2}}$. We use this to construct a MCE to demonstrate that a trimodal vertical cloud distribution can adequately simulate the observed

CRE, with ambiguity in the distribution of low- versus mid-level clouds. The measurements provide a much stronger constraint to high clouds.

In addition, clouds, even if they do not change their albedo, alter the Earth's climate sensitivity, i.e., its warming in response to a CO_2 doubling. On one hand, they mask the radiative forcing by about $0.7\,\mathrm{W\,m^{-2}}$, thus decreasing the climate sensitivity by about $15\,\%$. On the other hand, they both mask and unmask the radiative response to warming, with the latter slightly more dominant on average, so as to increase the expected response by $0.2\,\mathrm{W\,m^{-2}\,K^{-1}}$, an increase that is almost exactly canceled when the effect of clouds on the masking of surface albedo is considered. Our calculations thus suggest that in the absence of changes in cloud albedo, the difference between the all sky and clear-sky climate sensitivity is about zero.

275

Code availability. `konrad v1.0.2` is available on https://doi.org/10.5281/zenodo.7438306.

280

Author contributions. The presented concepts and ideas have been developed jointly by all authors. LK has performed the analysis, created the figures, and written the original draft. BS has created the schematic of the cloud masking. MB has developed the algorithm to compute the all-sky fluxes.

Competing interests. We are not aware of any competing interests.

References

Bony, S., Stevens, B., Coppin, D., Becker, T., Reed, K. A., Voigt, A., and Medeiros, B.: Thermodynamic control of anvil cloud amount, Proc. Natl. Acad. Sci. U.S.A., 113, 8927–8932, https://doi.org/10.1073/pnas.1601472113, 2016.

Bourdin, S., Kluft, L., and Stevens, B.: Dependence of Climate Sensitivity on the Given Distribution of Relative Humidity, Geophys Res Lett, 48, https://doi.org/10.1029/2021GL092462, 2021.

Ceppi, P., Brient, F., Zelinka, M. D., and Hartmann, D. L.: Cloud feedback mechanisms and their representation in global climate models, WIREs Clim Change, 8, https://doi.org/10.1002/wcc.465, 2017.

Colman, R.: A comparison of climate feedbacks in general circulation models, Climate Dynamics, 20, 865–873, https://doi.org/10.1007/s00382-003-0310-z, 2003.

Dacie, S., Kluft, L., Schmidt, H., Stevens, B., Buehler, S. A., Nowack, P. J., Dietmüller, S., Abraham, N. L., and Birner, T.: A 1D RCE study of factors affecting the tropical tropopause layer and surface climate, Journal of Climate, 32, 6769–6782, 2019.

Feng, J., Paynter, D., and Menzel, R.: How a Stable Greenhouse Effect on Earth Is Maintained Under Global Warming, Journal of Geophysical Research: Atmospheres, 128, e2022JD038 124, https://doi.org/https://doi.org/10.1029/2022JD038124, e2022JD038124 2022JD038124, 2023.

Forster, P., Storelvmo, T., Armour, K., Collins, W., Dufresne, J.-L., Frame, D., Lunt, D., Mauritsen, T., Palmer, M., Watanabe, M., Wild, M., and Zhang, H.: The Earth's Energy Budget, Climate Feedbacks, and Climate Sensitivity, in: Climate Change 2021: The Physical Science Basis. Contribution of Working Group I to the Sixth Assessment Report of the Intergovernmental Panel on Climate Change, edited by Masson-Delmotte, V., Zhai, P., Pirani, A., Connors, S., Péan, C., Berger, S., Caud, N., Chen, Y., Goldfarb, L., Gomis, M., Huang, M., Leitzell, K., Lonnoy, E., Matthews, J., Maycock, T., Waterfield, T., Yelekçi, O., Yu, R., and Zhou, B., p. 923–1054, Cambridge University Press, Cambridge, United Kingdom and New York, NY, USA, https://doi.org/10.1017/9781009157896.009, 2021.

Gloeckner, H. M., Kluft, L., Schmidt, H., and Stevens, B.: Estimates of the Global Clear-Sky Radiative Feedback Strength from Reanalysis Data, Geophysical Research Letters, https://doi.org/10.22541/essoar.173120498.80588022/v1, in press 2025.

Hartmann, D. L. and Short, D. A.: On the Use of Earth Radiation Budget Statistics for Studies of Clouds and Climatel, Journal of the Atmospheric Sciences, 37, 1233–1250, 1980.

Ingram, W.: A Very Simple Model for the Water Vapour Feedback on Climate Change: A Simple Model for Water Vapour Feedback on Climate Change, Quarterly Journal of the Royal Meteorological Society, 136, 30–40, https://doi.org/10.1002/qj.546, 2010.

Jeevanjee, N.: Climate sensitivity from radiative-convective equilibrium: A chalkboard approacha), American Journal of Physics, 91, 731–745, https://doi.org/10.1119/5.0135727, 2023.

Jeevanjee, N., Seeley, J. T., Paynter, D., and Fueglistaler, S.: An Analytical Model for Spatially Varying Clear-Sky CO2 Forcing, Journal of Climate, 34, 9463–9480, https://doi.org/10.1175/JCLI-D-19-0756.1, 2021.

Kluft, L., Dacie, S., Buehler, S. A., Schmidt, H., and Stevens, B.: Re-Examining the First Climate Models: Climate Sensitivity of a Modern Radiative–Convective Equilibrium Model, Journal of Climate, 32, 8111–8125, https://doi.org/10.1175/JCLI-D-18-0774.1, 2019.

Kluft, L., Dacie, S., Brath, M., Buehler, S. A., and Stevens, B.: Temperature-Dependence of the Clear-Sky Feedback in Radiative-Convective Equilibrium, Geophysical Research Letters, 48, https://doi.org/10.1029/2021GL094649, 2021.

Koll, D. D. B. and Cronin, T. W.: Earth's outgoing longwave radiation linear due to H_2O greenhouse effect, Proc. Natl. Acad. Sci. U.S.A., 115, 10 293–10 298, https://doi.org/10.1073/pnas.1809868115, 2018.

Koll, D. D. B., Jeevanjee, N., and Lutsko, N. J.: An Analytic Model for the Clear-Sky Longwave Feedback, Journal of the Atmospheric Sciences, 80, 1923 – 1951, https://doi.org/10.1175/JAS-D-22-0178.1, 2023.

Loeb, N. G., Doelling, D. R., Wang, H., Su, W., Nguyen, C., Corbett, J. G., Liang, L., Mitrescu, C., Rose, F. G., and Kato, S.: Clouds and the Earth's Radiant Energy System (CERES) Energy Balanced and Filled (EBAF) Top-of-Atmosphere (TOA) Edition-4.0 Data Product,
325 Journal of Climate, 31, 895–918, https://doi.org/10.1175/JCLI-D-17-0208.1, publisher: American Meteorological Society Section: Journal of Climate, 2018.

McKim, B. A., Jeevanjee, N., and Vallis, G. K.: Joint Dependence of Longwave Feedback on Surface Temperature and Relative Humidity, Geophysical Research Letters, 48, e2021GL094 074, https://doi.org/https://doi.org/10.1029/2021GL094074, e2021GL094074 2021GL094074, 2021.

330 Mlawer, E. J., Taubman, S. J., Brown, P. D., Iacono, M. J., and Clough, S. A.: Radiative transfer for inhomogeneous atmospheres: RRTM, a validated correlated-k model for the longwave, J. Geophys. Res., 102, 16 663–16 682, https://doi.org/10.1029/97JD00237, 1997.

Myhre, G., Highwood, E. J., Shine, K. P., and Stordal, F.: New Estimates of Radiative Forcing Due to Well Mixed Greenhouse Gases, Geophysical Research Letters, 25, 2715–2718, https://doi.org/10.1029/98GL01908, 1998.

Pincus, R., Barker, H. W., and Morcrette, J.-J.: A fast, flexible, approximate technique for computing radiative transfer in inhomogeneous
335 cloud fields, Journal of Geophysical Research: Atmospheres, 108, https://doi.org/https://doi.org/10.1029/2002JD003322, 2003.

Pistone, K., Eisenman, I., and Ramanathan, V.: Observational Determination of Albedo Decrease Caused by Vanishing Arctic Sea Ice, Proceedings of the National Academy of Sciences, 111, 3322–3326, https://doi.org/10.1073/pnas.1318201111, 2014.

Raghuraman, S. P., Medeiros, B., and Gettelman, A.: Observational Quantification of Tropical High Cloud Changes and Feedbacks, Journal of Geophysical Research: Atmospheres, 129, e2023JD039 364, https://doi.org/https://doi.org/10.1029/2023JD039364, e2023JD039364
340 2023JD039364, 2024.

Ramanathan, V., Cess, R. D., Harrison, E. F., Minnis, P., and Barkstrom, B. R.: Cloud-Radiative Forcing and Climate: Results from the Earth Radiation Budget Experiment, Science, 243, 57–63, 1989.

Roemer, F. E., Buehler, S. A., Brath, M., Kluft, L., and John, V. O.: Direct observation of Earth's spectral long-wave feedback parameter, Nature Geoscience, 16, 416–421, 2023.

345 Romps, D. M.: An Analytical Model for Tropical Relative Humidity, Journal of Climate, 27, 7432 – 7449, https://doi.org/10.1175/JCLI-D-14-00255.1, 2014.

Romps, D. M.: Climate Sensitivity and the Direct Effect of Carbon Dioxide in a Limited-Area Cloud-Resolving Model, Journal of Climate, 33, 3413–3429, https://doi.org/10.1175/JCLI-D-19-0682.1, 2020.

Seeley, J. T. and Jeevanjee, N.: H_2O Windows and CO_2 Radiator Fins: A Clear-Sky Explanation for the Peak in Equilibrium Climate
350 Sensitivity, Geophys Res Lett, 48, https://doi.org/10.1029/2020GL089609, 2021.

Soden, B. J. and Held, I. M.: An Assessment of Climate Feedbacks in Coupled Ocean–Atmosphere Models, Journal of Climate, 19, 3354–3360, https://doi.org/10.1175/JCLI3799.1, 2006.

Soden, B. J., Held, I. M., Colman, R., Shell, K. M., Kiehl, J. T., and Shields, C. A.: Quantifying Climate Feedbacks Using Radiative Kernels, Journal of Climate, 21, 3504 – 3520, https://doi.org/10.1175/2007JCLI2110.1, 2008.

355 Stevens, B. and Kluft, L.: A Colorful Look at Climate Sensitivity, Atmospheric Chemistry and Physics, 23, 14 673–14 689, https://doi.org/10.5194/acp-23-14673-2023, 2023.

Yoshimori, M., Lambert, F. H., Webb, M. J., and Andrews, T.: Fixed Anvil Temperature Feedback: Positive, Zero, or Negative?, Journal of Climate, 33, 2719–2739, https://doi.org/10.1175/JCLI-D-19-0108.1, 2020.

Zelinka, M. D. and Hartmann, D. L.: Why is longwave cloud feedback positive?, Journal of Geophysical Research: Atmospheres, 115,

360   https://doi.org/https://doi.org/10.1029/2010JD013817, 2010.

Quantity	Unit	Value
Effective radius (liquid)	μm	10
Effective radius (ice)	μm	50
High cloud fraction	%	1–35
Mid cloud fraction	"	"
Low cloud fraction	"	"
IWP high cloud	$g\,m^{-2}$	2–75
LWP mid-level cloud	"	20–200
LWP low cloud	"	2–200

Table 1. Possible value range for physical and optical cloud parameters in the MCE. Numbers which do not change between rows are marked with a ".

	3 layers, percentiles			no mid, percentiles			no low, percentiles		
Quantity	5th	50th	95th	5th	50th	95th	5th	50th	95th
Cloud fraction									
high-level	0.13	0.18	0.27	0.16	0.21	0.30	0.12	0.16	0.23
mid-level	0.02	0.20	0.33	–	–	–	0.02	0.18	0.33
low-level	0.03	0.17	0.31	0.18	0.24	0.33	–	–	–
Condensate burden $(g\,m^{-2})$									
high-level	12.39	38.42	66.72	12.77	38.38	66.74	12.41	40.76	67.53
mid-level	31.74	113.3	192.4	–	–	–	125.5	164.7	197.1
low-level	18.1	97.1	187.6	54.4	117.7	189.3	–	–	–

Table 2. Plausible value range for cloud amounts in the MCE.